Journal of Hydrology: Regional Studies 63 (2026) 103009

Contents lists available at ScienceDirect

Journal of Hydrology: Regional Studies

journal homepage: www.elsevier.com/locate/ejrh

A nonstationary framework for hydrological drought assessment in Iran

Sedigheh Anvari [a,*], Jesper Rydén [b], Ameneh Mianabadi [a]

[a] Department of Ecology, Institute of Science and High Technology and Environmental Science, Graduate University of Advanced Technology, Kerman, Iran

[b] Unit of Applied Statistics and Mathematics, Department of Energy and Technology, Swedish University of Agricultural Sciences, Uppsala, Sweden

ARTICLE INFO

Keywords:
Drought
Nonstationary
SRI
NSRI
Hydro-Meteorological Covariates
GAMLSS

ABSTRACT

Study region: The Halil-Rud Basin in Iran, a semi-arid watershed, has been increasingly affected by climate change over the past decades, impacting hydrological processes and water resource

Study focus: This study introduces a Nonstationary Standardized Runoff Index (NSRI) to enhance hydrological drought assessment in the Halil-Rud Basin for the period 1980–2019. Using the GAMLSS framework with a time-varying gamma distribution, NSRI models incorporate linear relationships between runoff and hydroclimatic covariates, including precipitation, temperature, potential evapotranspiration, and antecedent runoff. Four models—one stationary (M0) and three nonstationary (M1–M3)—were evaluated across 14 covariate combinations using monthly runoff data from three stations (Pole-Baft, Meidan, Kenaroyeh), comparing drought severity, duration, and intensity.

New hydrological insights for the region: Results indicate that nonstationary models consistently outperform the stationary baseline, with M2 (temperature and antecedent runoff) providing the best fit. Analysis of S/NS drought indices along the Halil-Rud Basin reveals that NSRI more accurately captures spatiotemporal drought variability, especially in downstream regions affected by anthropogenic influences. Compared to SSRI, NSRI moderates extreme drought estimates, highlighting the risk of overestimation when using stationary assumptions. These findings demonstrate the value of nonstationary modeling for robust drought monitoring and adaptive water resource management in semi-arid regions.

1. Introduction

As a persistent and inherent aspect of our climate, drought exerts significant influence on global economic stability, social structures, and ecological health (Wilhite, 2000; Mishra and Singh, 2010; Moghaddasi et al., 2022; Anvari et al., 2019).

Drought is a complex and multifaceted natural phenomenon that typically emerges from a deficit in precipitation, leading to diminished soil moisture through the processes of evapotranspiration and a reduction in river flow. These conditions can have devastating effects on both plant health and human livelihoods. Drought is generally defined as a "deficiency of rainfall resulting in water scarcity" or as a "prolonged period of abnormally dry weather, characterized by scant rainfall and leading to a considerable hydrological imbalance" (Heim, 2002; Li et al., 2013). Additionally, drought is frequently associated with deficiencies in streamflow,

* Corresponding author.
E-mail addresses: anvari.t@gmail.com, s.anvari@kgut.ac.ir (S. Anvari), jesper.ryden@slu.se (J. Rydén), amianabadi@kgut.ac.ir (A. Mianabadi).

https://doi.org/10.1016/j.ejrh.2025.103009
Received 11 October 2025; Received in revised form 13 November 2025; Accepted 30 November 2025
Available online 13 December 2025

soil moisture, agricultural productivity, and various socioeconomic factors (e.g., Huang et al., 2016).

While a precise definition of drought remains challenging to establish, several indices have been developed to effectively monitor drought conditions. Among the most widely used tools are the Palmer Drought Severity Index (PDSI) (Palmer, 1965), the Standardized Precipitation Index (SPI) (McKee et al., 1993), the Reconnaissance Drought Index (RDI) (Tsakiris and Vangelis, 2005), and the Standardized Precipitation Evapotranspiration Index (SPEI) (Vicente-Serrano et al., 2010). These indices are primarily employed to assess precipitation-based meteorological droughts. Furthermore, the Standardized Runoff Index (SRI) is utilized to monitor hydrological droughts associated with runoff and streamflow (Shukla and Wood, 2008). For the evaluation of agricultural drought, the Standardized Soil Moisture Index (SSI) and the Agricultural Standardized Precipitation Index (aSPI) are commonly applied (Hao and AghaKouchak, 2013). Moreover, numerous drought indices have been devised to account for various climatic variables. Notable examples include the Standardized Precipitation-Evapotranspiration Index (SPEI), the Vegetation Drought Response Index (VegDRI) (Brown et al., 2008), the Reconnaissance Drought Index (RDI) (Tsakiris and Vangelis, 2005), the Multivariate Standardized Drought Index (MSDI) (Hao and AghaKouchak, 2013), and the Evaporative Stress Index (ESI) (Anderson et al., 2007). For a comprehensive review of drought indices, readers are encouraged to consult the works of Mishra and Singh (2010).

Notably, the SPI has gained prominence due to its computational simplicity, emerging as the most widely accepted and robust index in drought monitoring. It is often regarded as a fundamental component of an effective drought assessment system (Hayes et al., 2011; Pasho et al., 2011). The SPI can be calculated across various time scales and is particularly adept at statistically comparing drought severity both temporally and spatially (Bonaccorso et al., 2003).

As the frequency and severity of droughts increase due to climate change (Dai, 2011; Mishra and Singh, 2009; Moghaddasi et al., 2022; Mohammadi et al., 2024), the need for an effective drought monitoring system becomes more crucial in the context of changing hydro-climatic conditions. Given the ongoing shifts in climate, it is vital to reassess, rethink, and enhance the computational aspects of existing drought indices. Typically, commonly used drought indices- including meteorological, hydrological, agricultural, and socio-economic measures- fail to account for environmental changes arising from climate change, anthropogenic influences, and human activities. This non-stationarity (NS) of drought indices presents significant challenges for researchers and practitioners (Sun et al., 2020; Das et al., 2021; Anvari and Moghaddasi, 2024; Delavar et al., 2024; Anvari and Rydén, 2025). To date, efforts have focused on developing drought indices that operate under conditions of non-stationarity (Li et al., 2015; Wang et al., 2015; Rashid and Beecham, 2019; Bazrafshan et al., 2022).

In the investigation of non-stationary drought indices (NSDI), the initial task is to identify a suitable covariate that effectively captures the trends in hydro-climatic variables. Following this, it is essential to select an appropriate statistical modeling tool for NS analysis. A prominent choice for researchers is the Generalized Additive Models for Location, Scale, and Shape (GAMLSS) package, which is not only widely utilized but also freely accessible (Rigby and Stasinopoulos 2005, Stasinopoulos and Rigby (2007), Rydén (2019); Delavar et al., 2024).

Since the 1990s, research on NS drought indices (NSDI) has gained momentum, beginning with Russo et al. (2013), who introduced the Standardized non-stationary Precipitation Index (SnsPI) using a NS Gamma distribution within the SPI framework. Wang et al. (2015) further advanced this field by proposing a time-dependent Standardized Precipitation Index (SPIt) for the Luanhe River Basin, modeling NS through a Gamma distribution with a time-dependent location parameter. Their findings indicated that the NS Gamma distribution generally outperforms its stationary counterpart in fitting precipitation series. Bazrafshan and Hejabi (2018) developed the Non-Stationary RDI (NRDI) to enhance drought monitoring across fifteen meteorological stations in Iran (1951–2014) using the GAMLSS algorithm, revealing significant differences between NRDI and traditional RDI, particularly for time windows exceeding six months. In the study of the upper Heihe River basin, China, Sun et al. (2020) introduced a non-stationary Standardized Runoff Index (NSRI) using a NS Gamma distribution within the GAMLSS framework. By integrating relevant covariates influencing the NS characteristics of runoff, they demonstrated that NS models offer enhanced robustness over stationary ones, with the model incorporating two covariates performing most effectively. Das et al. (2021) developed the NS Standardized Precipitation Index (NSPI) and Non-stationary Reconnaissance Drought Index (NRDI) by incorporating large-scale climatic oscillations, utilizing the GAMLSS model across 103 grid points in Maharashtra, India. Their results demonstrated that NS modeling significantly outperforms stationary approaches at various drought scales. Similarly, Bazrafshan et al. (2022) created a Non-stationary SPEI (NSPEI) using monthly precipitation and temperature data from 32 weather stations in Iran, employing a non-stationary log-logistic probability distribution. This model treated the location parameter as a multivariable function of time and climate indices as covariates, with findings indicating that the NS log-logistic distributions consistently surpassed stationary models at nearly all stations (Bazrafshan et al., 2022).

Historical evidence highlights that Iran has experienced long-term and devastating droughts over the centuries. Notably, the severe famines during 1870–1872 and 1917–1919, triggered by drought conditions, jeopardized water and food security across the country and resulted in the loss of half the population (Bazrafshan, 2017; Bazrafshan and Hejabi, 2018; Delavar et al., 2024; Anvari et al., 2023; Anvari and Rydén, 2025). Bazrafshan (2017) documented that between 1894 and 2010, Iran, with an average annual precipitation of 254 mm, endured 23 drought events lasting from 1 to 10 years. Among these, the 2008–2010 and 1998–2002 droughts, with total precipitation deficits of 176.1 mm and 180.4 mm, respectively, were identified as the most severe and widespread.

The standardized runoff index (SRI) is one of the most widely used indices in the assessment of hydrological drought worldwide (Jiang et al., 2019). Proposed by Shukla and Wood (2008), the SRI is based on the theory of the SPI developed by McKee et al. (1993). Its broad acceptance stems from its simplicity in calculation, the minimal data requirements, and its ability to assess hydrological

drought across different time scales. However, the stationarity assumption of the SRI is frequently violated in the context of global warming and significant human disturbances (Xiong and Guo, 2004; Villarini et al., 2009; Liu et al., 2019).

This study aims to develop a Non-Stationary Standardized Runoff Index (NSRI) tailored to the context of Iran's changing climate. The novelty lies in modeling the non-stationarity of climate-related variables using both temporal and hydro-climatic covariates that influence the regional climate dynamics. The proposed NSRI is evaluated against its stationary counterpart in terms of both temporal and spatial drought characteristics. Furthermore, its effectiveness in capturing the impact of the most severe drought period across Iran is assessed relative to the stationary SRI (SSRI). Methodologically, the study contributes to the statistical modeling literature by exploring NS parameterization within the GAMLSS framework, supported by model comparison using the Akaike Information Criterion (AIC) and diagnostic tools such as worm plots.

It should be noted that the present study primarily focuses on trend-driven non-stationarity, which is modeled through smooth covariate effects within the GAMLSS framework. This approach allows for the representation of gradual and continuous changes in the statistical behavior of runoff over time, thereby capturing the influence of evolving hydroclimatic conditions across the Halil-Rud Basin. In this context, we assume that these temporal variations can be reasonably approximated by linear trends in the covariates, reflecting long-term, systematic changes rather than abrupt fluctuations. Furthermore, we examine the spatio-temporal variability of both SSRI and NSRI, acknowledging that spatial heterogeneity arises from the geographical distribution of sites and the gradual transition of hydroclimatic variables from upstream to downstream areas. Based on previous studies of meteorological and hydrological drought monitoring in Iran (e.g., Morid et al., 2006; Naderi et al., 2022; Anvari et al., 2023), which have consistently demonstrated the superior performance of the gamma distribution, we assume that the gamma and non-stationary gamma (NS-gamma) distributions are suitable for modeling SSRI and NSRI, respectively.

The remainder of this paper is structured as follows: 2 provides an overview of the Halil-Rud River Basin and the data utilized. 3 outlines the methodological approach. 4 details the model development, presents the results, and offers a comprehensive analysis. Finally, 5 summarizes the main conclusions and proposes directions for future research.

2. Study area and datasets

2.1. Study area

The Halil-Rud river basin, situated in the subtropical monsoon region of Kerman Province, Iran, covers an area of approximately 22,255 km^2. The section of the basin up to the Jirof Dam, which is the focus of this paper, spans about 7224 km^2 (see Fig. 1).

Influenced by its geographical location and topography, the basin experiences an annual average temperature of 13°C. The maximum daily average temperature can reach up to 40°C at Kenaroyeh station located near the outlet of the basin. The long-term average annual precipitation in the basin is less than 225 mm (1993–2009), most of which is received between January and May, whereas precipitation is negligible between June and December. The Halil-Rud River is a significant watercourse in the province, particularly in terms of discharge, and it contributes to the feeding of the Jazmorian Wetland. The water released from the Halil-Rud River to the wetland is controlled by the Jiroft Dam at Kenaroyeh station (shown in Fig. 1). During the period from 1993 to 2009, the maximum and minimum annual average discharges were 33 m^3 /s in 1995 and 0.71 m^3 /s in 2007, respectively. Annual potential evaporation (PE) at the Baft synoptic station ranges from 2039 to 2569 mm, contributing to a low runoff coefficient of 0.12 (Mahmoodi et al., 2020; Eslami et al., 2022).

2.2. Data collection and analysis

In this study, three distinct datasets were utilized to support the analysis:

a) Monthly precipitation and air temperature records from three synoptic stations located within the Halil-Rud Basin (Fig. 1),
b) Historical runoff data from three hydrometric stations, and
c) Gridded climate data derived from the Climatic Research Unit (CRU) database.

– **Station-based observations:** The station-based dataset comprises long-term meteorological and hydrological records spanning the period 1980–2019. Monthly precipitation and temperature data were obtained from three synoptic stations—Baft, Jiroft, and Kahnooj—provided by the Iran Meteorological Organization (IMO). In parallel, monthly runoff data were sourced from five hydrometric stations, namely Pole-Baft, Meidan, and Kenaroyeh, which are managed by the Iran Ministry of Energy. These observational datasets formed the basis for assessing regional hydroclimatic variability and served as critical inputs for the subsequent drought modeling framework.

Fig. 2 illustrates the 40-year time series of runoff data for the Kenaroyeh and Meidan stations, presented sequentially.

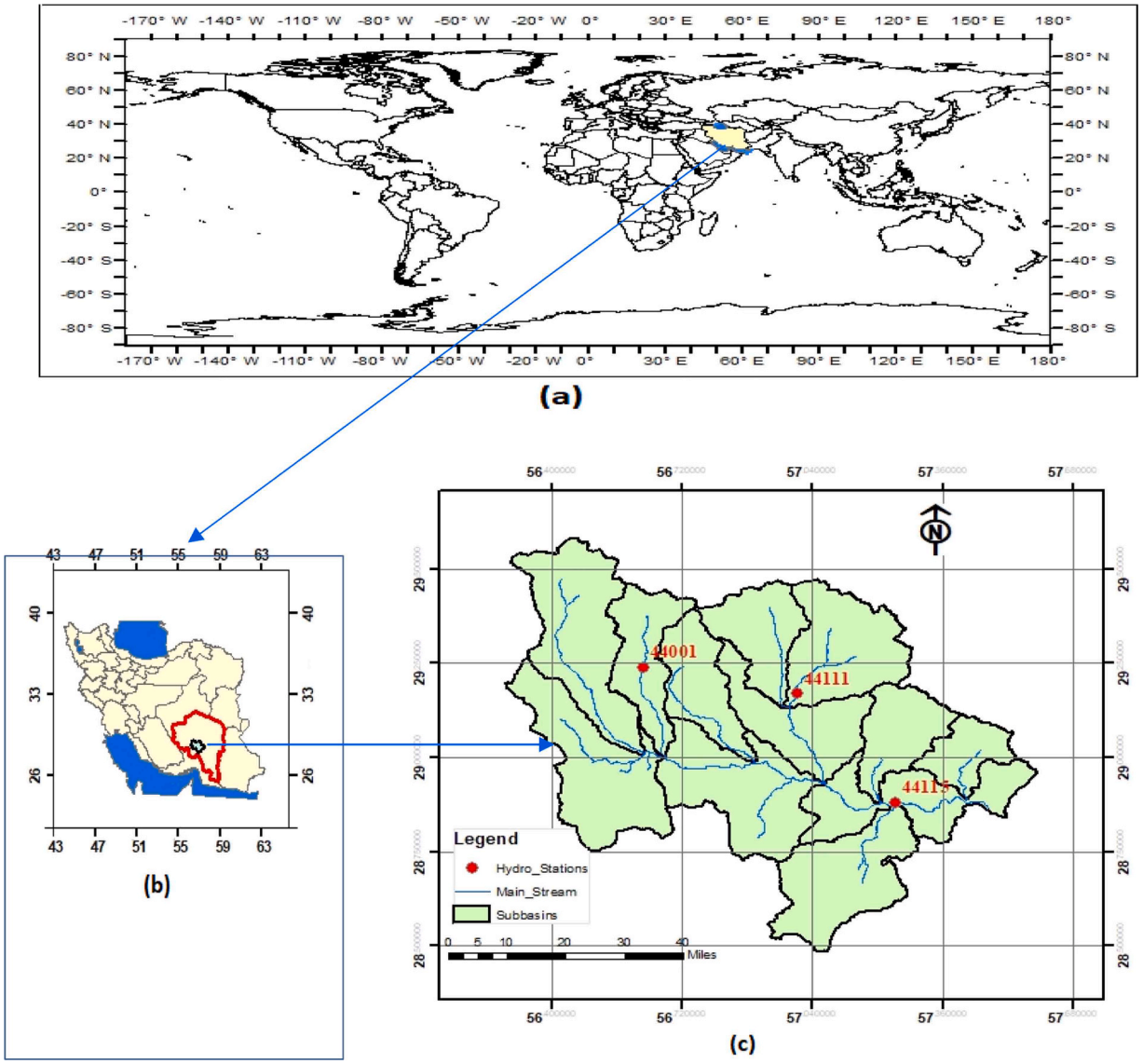

Fig. 1. Multi-scale geographic overview depicting: (a) Iran's global position, (b) the study area within Iran—Kerman Province, and (c) the spatial layout of selected hydrometric stations.

Climate Research Unit (CRU) data: As previously mentioned, this study utilized weather data, including precipitation and temperature (mean, maximum, and minimum), extracted from the CRU database. The CRU produced time series of monthly climate variables from 1901 to 2019 with a 0.5-degree spatial resolution (New et al., 1999; Mitchell and Jones, 2005). These monthly gridded data were generated from ground-based climate variables over land and interpolated using the Inverse Distance Weighted (IDW) method. The data can be accessed from the CRU data website.[1] The accuracy of the CRU gridded data against observational point-based data was also measured using some evaluation criteria like root mean square error (RMSE) and coefficient of determination (R^2) for the period 1980–2019. Results showed both temat selected synoptic stations

3. Materials and methods

As illustrated in Fig. 3. flowchart of the methodology in current paper, ensures a comprehensive approach to analyzing drought scenarios under S and NS conditions, integrating trend analysis and statistical modeling for robust results.

The research begins with the collection of meteorological and hydrometric data from 1980 to 2019. The meteorological data

[1] https://crudata.uea.ac.uk/cru/data

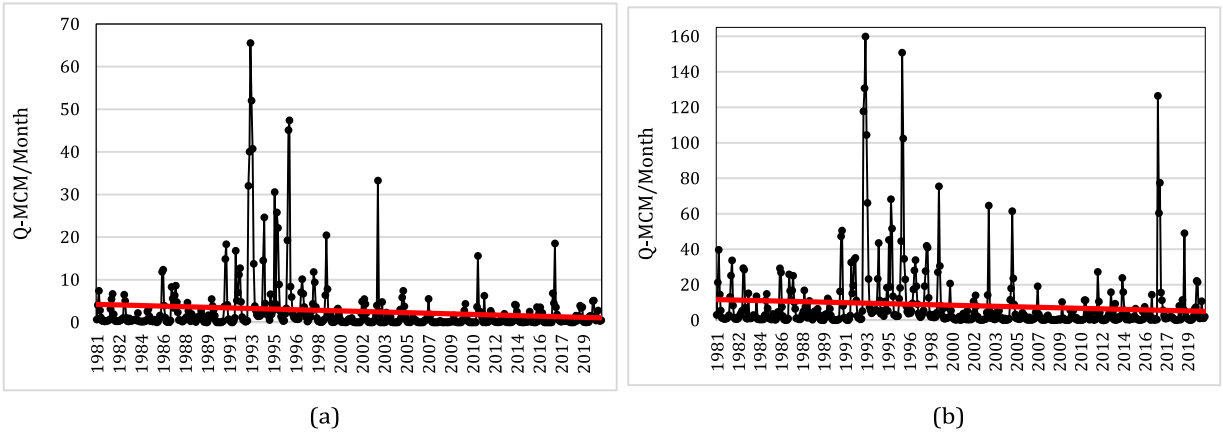

Fig. 2. The 40-year time series of runoff data for (a) Meidan and (b) Kenaroyeh stations.

undergo preprocessing and analysis to determine their correlation with runoff time series from hydrometric stations. These correlations are essential for developing NS covariate scenarios within the GAMLSS framework. Concurrently, hydrometric time series are assessed for non-stationarity using the Mann-Kendall (MK) trend test and the Augmented Dickey-Fuller (ADF) test. Based on the most statistically significant covariate scenarios, both S/NS drought models are constructed by fitting Gamma probability distributions. Next, the Stationary SRI (SSRI) and its NS variant (NSRI) are calculated to characterize drought events in terms of frequency, duration, and severity. A comparative analysis of SSRI and NSRI follows to identify the most effective index for capturing hydrological drought dynamics in the study area.

3.1. The Mann–Kendall Trend test

The non-parametric Mann-Kendall (M-K) test is a statistical method utilized for detecting trends in data time series. This test is used to identify whether the median of a data time series changes over time (Mann, 1945; Kendall 1976). In the M-K test, the H0 (null hypothesis) and H1 (alternative hypothesis) correspond to data time series without and with trend, respectively. The following relationships are used: The H0 is rejected when the test statistic is meaningfully different from zero at 5 % significance level, i.e., if $|ZM= > 1.96$, then H0 is rejected which means that trend has been detected in the time series.

3.2. Stationary test by Augmented Dickey–Fuller (ADF)

After confirming the presence of a trend in the data, the Augmented Dickey–Fuller (ADF) test (Dickey and Fuller, 1979) was employed to assess the stationarity of the series. The ADF test is an extension of the original Dickey–Fuller test (Dickey and Fuller, 1979), designed to account for more complex data structures by including lagged difference terms. In this study, a 12-month cumulative runoff time series from 1980 to 2019 was used for the NS analysis of the SSRI. The ADF test was applied to this cumulative dataset to evaluate its stationarity. To determine stationarity, the calculated ADF test statistic was compared against the critical value at a 5 % significance level. If the test statistic exceeds the critical value, the null hypothesis—that the series is NS—is not rejected, indicating non-stationarity in the time series.

3.3. Stationary Standardized Runoff Index (SSRI)

Analogous to the SPI (McKee et al., 1993), the SRI (Shukla andWood, 2008), is one of the most widely used indices worldwide in the hydrological drought assessment (Jiang et al., 2019; Sun et al., 2020). Given that the traditional SRI is computed assuming stationarity, we will now denote it as the Stationary SRI (SSRI).

SRI remains the most broadly accepted index due to being simple to calculate, the limited data required, and the different time scales of hydrological drought assessed. To obtain this index, fit the runoff series for a certain period by using Gamma distribution firstly and then transform it into a standard normal distribution through an equal probability transformation. The specific calculation process is as follows:

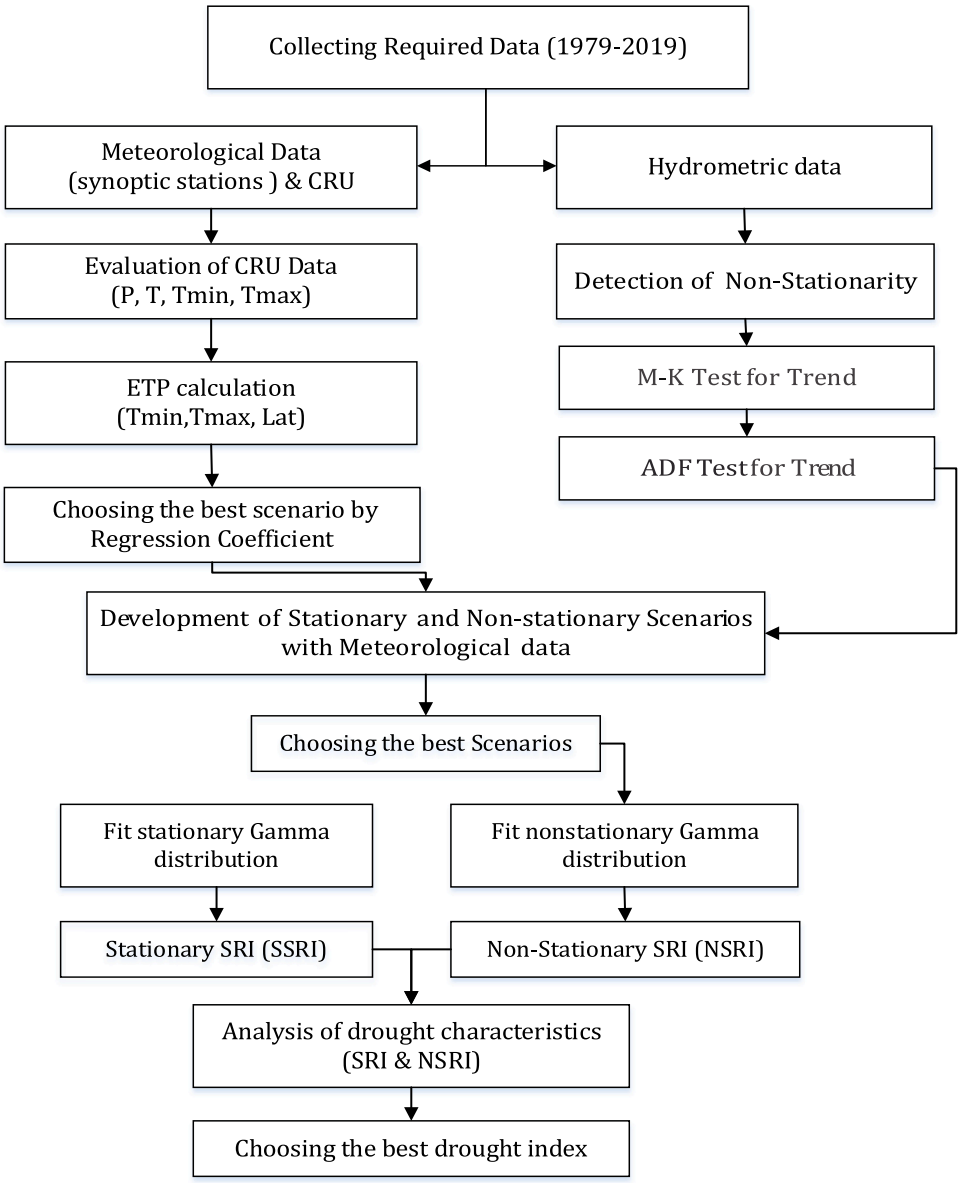

Fig. 3. Development of a stationary /non-stationary SRI (SSRI and NSRI).

Runoff data aggregation: Monthly runoff series from the three hydrometric stations (Pole-Baft, Meidan, and Kenaroyeh) covering 1980–2019 were first collected. Let x(n) represents the runoff data at the nth month. Fourty years (1980–2019) of runoff data are available here, thus n ranges from 1 to 648. For a given time scale of k months (a time scale of 12-month is considered here), the cumulative runoff xk(n) is calculated as:

$$x_k(n) = \sum_{i=n-k+1}^{n} x(i) \tag{1}$$

Fitting a two-parameter Gamma distribution, denoted as xk(n) ~ Gamma (μ, σ), which has been widely applied for hydrological drought indices (Morid et al., 2006; Wang et al., 2015; Sun et al., 2020):

$$f(x_k(n)|\mu,\sigma) = \frac{1}{(\sigma^2\mu)^{1/\sigma^2}} \quad \frac{(x_k(n))^{\frac{1}{\sigma^2}} - 1\exp\lfloor -(x_k(n))/\sigma^2\mu \rfloor}{\Gamma(1/\sigma^2)}, x_k(n) > 0 \tag{2}$$

where μ and σ are the location and scale parameters in Gamma, μ > 0 and σ> 0. Γ(.) is the mathematical Gamma function. The cumulative probability for a given time scale can be calculated as:

$$F(x_k \quad (n)) = \int_0^x f(x_k \quad (n)).dx \tag{3}$$

Converting cumulative probability to a standard normal distribution function

$$\mathrm{SRI} = \begin{cases} -\omega + \dfrac{c_0 \quad + c_1 \quad \omega + c_2 \quad \omega^2}{1 + d_1\omega + d_2 \quad \omega^2 + d_3 \quad \omega^3} \\ \omega = \sqrt{\ln\left[\dfrac{1}{F(x_k \quad (n)^2}\right]} \quad 0 \quad \leq F(x_k \quad (n) \quad \leq \quad 0.5 \\ -\omega + \dfrac{c_0 \quad + c_1 \quad \omega + c_2 \quad \omega^2}{1 + d_1\omega + d_2 \quad \omega^2 + d_3 \quad \omega^3} \\ \omega = \sqrt{\ln\left[\dfrac{1}{1 - F(x_k \quad (n)^2}\right]} \quad 0.5 \quad \leq F(x_k \quad (n) \quad \leq \quad 1 \end{cases} \tag{4}$$

where $c_0 = 2.515517$, $c_1 = 0.802853$, $c_2 = 0.010328$, $d_1 = 1.432788$, $d_2 = 0.189269$, and $d_3 = 0.001308$ (Shukla andWood, 2008). Negative SSRI values indicate dry periods (droughts), while positive values signify wet periods. For the last step, we followed in our work the implementation in base R of the inverse cumulative distribution of the normal distribution. This is also the implementation found in the R package SPEI.

4. Non-stationary SRI (NSRI)

4.1. Theory of NSRI construction

The SSRI model operates under the assumption that the parameters of the gamma distribution fitted to the 12-month cumulative series remain constant over time. In contrast, the NSRI applies an optimized NS model, allowing the distribution parameters to vary—either linearly or nonlinearly—with time or relevant external covariates.

Given the extended nature of hydrological time series—especially those spanning over 30 years—it is imperative to account for NS behavior to avoid misrepresenting drought characteristics (Russo et al., 2013). To this end, we adopted the Generalized Additive Models for Location, Scale, and Shape (GAMLSS) framework (Rigby and Stasinopoulos, 2001, 2005) to develop the NSRI. GAMLSS represents a flexible, distribution-based modeling approach that surpasses the constraints of traditional generalized linear models (GLMs) and generalized additive models (GAMs) (Hastie and Tibshirani, 1987). Unlike its predecessors, GAMLSS enables the modeling of multiple distributional parameters—including location, scale, and shape—as linear, non-linear, or non-parametric functions of explanatory variables and/or random effects (Rigby and Stasinopoulos, 2005).

4.2. NSRI computation procedure

The following section outlines the expanded steps involved in constructing the NSRI:

- **Runoff data aggregation and distributional assumptions:** Monthly runoff data from 1980 to 2019 were aggregated to a 12-month timescale to form the cumulative runoff series series $x_k(t)$. Each series was modeled using a non-stationary (NS) Gamma distribution, where the location (μ) and scale (σ) parameters were expressed as linear functions of hydroclimatic covariates.
- **Model fitting and covariate selection using the GAMLSS framework:** To assess the direct influence of local hydrometeorological variables on drought dynamics in the Halil-Rud Basin, four covariates—precipitation (P), temperature (T), potential evapotranspiration (PET), and antecedent runoff (R)—were evaluated using Pearson correlation analysis. The Generalized Additive Models for Location, Scale, and Shape (GAMLSS) framework was applied to capture non-stationarity in the aggregated runoff data, allowing μ and σ to vary linearly with selected covariates. The Rigby–Stasinopoulos (RS) algorithm ensured robust parameter estimation for the NS Gamma distribution. Three base models (M1–M3) were developed to represent different covariate combinations, resulting in 14 NS configurations by varying the covariate inputs for μ and σ. All models were fitted using penalized likelihood estimation, and their performance was compared using the Akaike Information Criterion (AIC; Akaike, 1974). For each hydrometric station, the model with the lowest AIC was identified as the optimal NSRI specification.
- **NSRI Computation**:After determining the best-fitting Gamma distribution for each station and month, NSRI values were derived by transforming observed runoff into standardized normal scores using the fitted cumulative distribution function (CDF). This process mirrors traditional SRI computation but employs a covariate-driven, time-varying distribution instead of a stationary one. In GAMLSS, the cumulative runoff xk(n) is modeled as xk(n) ~ Gamma (μ_n, σ_n). It is assumed that the changes of runoff with covariates obey the following distribution parameters:

$$\mu_n = a_0 \quad + \sum_{i=1}^{I} a_i z_{i(n)} \tag{5}$$

$$\sigma_n = b_0 + \sum_{i=1}^{I} b_i \quad z_{i(n)} \tag{6}$$

where μ_n and σ_n are the location and scale parameters in NS Gamma distribution, a_0 and b_0 are constant terms, z_i (i = 1, 2,…, I) is the covariate, and I is the number of covariates. Here, four variables are selected as alternative covariates, namely precipitation (P), temperature (T), potential evapotranspiration (PET) and antecedent runoff (R).

- **Validation and comparison**: The NSRI was compared against the stationary SRI (SSRI) using metrics such as drought severity, duration, and intensity. Time series plots and drought event analyses were used to assess the indices' responsiveness to hydro-climatic variability and anthropogenic influences.

The NSRI is analogous to SSRI since in both cases cumulative probabilities are converted into standard normal values, and similar drought-level standards for both indices are recommended (Guttman, 1999). Positive NSRI values in Table 2 indicate wet conditions, while negative values indicate dry conditions. Similarly to SSRI, a higher NSRI value signifies wetter conditions, and a lower value indicates drier conditions.

4.3. Evaluation criteria

Akaike Information Criterion (AIC) weighs up the goodness of fit of a model (Akaike, 1974). It is the most widely used model selection criterion and is defined as:

$$\mathrm{AIC} = -2 \quad (\mathrm{llh}) + 2K \tag{7}$$

where K is the number of estimated parameters and llh is the maximum value of the likelihood function for the model. The minimum AIC value corresponds to the best statistical model (Katz, 2010). The AIC was used for the selection of significant covariates.

AIC is a comparative measure, its actual value when comparing two models has no interpretation. When considering several options, the difference in AIC, ΔAIC say, is of interest to assess. Rules of thumbs have then been established (Burnham and Anderson, 2004); a too small difference in AIC might not be of practical interest. We here give a summary of differences and related conclusions:

- $\Delta\mathrm{AIC} \leq 2$: models have substantial support and are considered statistically indistinguishable
- $4 \leq \Delta\mathrm{AIC} \leq 7$: models have considerably less support
- $\Delta\mathrm{AIC} > 10$: models have essentially no support compared to the best model

4.4. Drought characteristics

The characteristics of drought are commonly delineated by their severity, duration, and frequency. The theory of runs, a probabilistic methodology introduced by Yevjevich (1967), is widely employed to derive these drought characteristics based on indices such as the SPI and the Standardized Precipitation Evapotranspiration Index (SPEI) (McKee et al., 1993; Vicente-Serrano et al., 2010). This methodology is extensively utilized to compute the severity, duration, and frequency of drought events by establishing a definitive threshold level (Yevjevich, 1967; Guttman, 1998).

In this study, the run-theory methodology was applied to delineate drought conditions using the SSRI and the NSRI. According to this theoretical framework, drought severity is quantified as the cumulative sum of SSRI or NSRI values falling below the established threshold. Drought duration is defined as the continuous period during which the SSRI or NSRI remains below this threshold, while drought frequency denotes the number of times the index crosses below this threshold (Gan et al., 2023; Hao and AghaKouchak, 2013). Duration is considered as a discrete random variable and in the recent study discrete distribution is fitted to the drought duration time series (Sarhadi et al., 2016)

Table 1
Hydrological and meteorological stations in the Halil-Rud River basin.

Station Type	Station Name	Code	Longitude & Latitude	Altitude (m)
Hydrometric Stations	Pole-Baft	44–001	56.63(°E), 29.24(°N)	2270
	Meidan	44–111	57.01 (°E), 29.17 (°N)	1915
	Kenaroyeh	44–115	57.24 (°E), 28.88 (°N)	1410
Synoptic Stations	Baft (Upstream)	40853	56.58 (°E), 29.23 (°N)	2280
	Jiroft-Miandeh (Downstream)	40866	57.80 (°E), 28.58 (°N)	722
	Kahnooj (Downstream)	40877	57.70 (°E), 27.96 (°N)	470

Table 2
Drought-level standards and the threshold values.

Index value	Category
> 2.00	Extreme wet
1.99–1.50	Very wet
1.49–1.00	Moderate wet
0.99–0.00	Near normal
0.00 to −0.99	Mild drought
-1.00 to - 1.49	Moderate drought
-1.50 to −1.99	Severe drought
≥ 2.00	Extreme drought

5. Results and discussion

5.1. Trend and stationary analysis

In this study, the SSRI was calculated on a 12-month timescale to align with the management practices of Iran's water resources, which are based on a water-year scale (i.e., October of the current year to September of the following year) (Raziei et al., 2008). The 12-month cumulative runoff time series data, spanning 1980–2019, were subjected to trend and stationarity tests using the MK method and ADF test. For these analyses, the 'trend' and 'tseries' packages in R were employed to compute P-values, trends, and Dickey-Fuller statistics directly. The MK test was conducted to evaluate the significance of trends at a 5 % significance level, as outlined in Table 3.

As demonstrated in Table 3, the p-values from the MK test for all stations are less than the 5 % significance level. Consequently, we reject the null hypothesis (which posits no trend) and accept the alternative hypothesis. To quantify the magnitude of this trend, Sen's slope was utilized, with the average slope across the selected stations calculated to be approximately −0.011, reflecting a decreasing trend. Notably, all three stations within the Halil-Rud basin exhibited a statistically significant decreasing trend in runoff time series data at the 5 % significance level, as indicated in Table 3. Moreover, the calculated p-values for ADF test during all selected months are greater than the (5 %) significance level, and so it is concluded that the null hypothesis of the NS state should be accepted.

As illustrated in Fig. 4, the Dickey–Fuller statistics for the Kenaroyeh, PoleBaft, and Meidan stations exceed the threshold of −3.5, while their corresponding P-values surpass 0.05. These findings confirm, at the 0.05 significance level, that the cumulative runoff series at these stations exhibit NS behavior. So, the development of the NSRI framework is imperative for accurately modeling these series.

5.2. Choosing the hydro-climate covariates

In regression-based model development, examining the correlation between the response variable and potential covariates is a critical preliminary step. To inform covariate selection for the NSRI formulation, Pearson correlation coefficients were computed between monthly runoff and four hydroclimatic variables-precipitation (P), temperature (T), potential evapotranspiration (PET), and antecedent runoff (R)-across three hydrometric stations: Baft, Jiroft-MianDeh, and Kahnooj.

Across all stations, runoff exhibited a positive correlation with precipitation, with coefficients ranging from approximately 0.20–0.37, indicating that higher rainfall generally leads to increased runoff. In contrast, both temperature and PET showed negative correlations with runoff (ranging from about –0.31 to –0.45), suggesting that increased heat and evaporative demand tend to reduce available surface runoff. Notably, antecedent runoff displayed a very strong positive correlation with current runoff, with coefficients exceeding 0.94 at all stations, highlighting the strong persistence and memory effects within the catchments.Overall, the correlation patterns were consistent across sites: moderate associations for precipitation, temperature, and ETP, and a markedly high correlation for antecedent runoff. These results provide a sound empirical basis for including these variables as potential covariates in the subsequent NS modeling framework.

6. GAMLSS results

To investigate seasonal runoff variability and its primary drivers, four models (M0–M3) were developed within a NS framework, each incorporating an increasing number of covariates. Model 0 (M0) serves as the baseline (stationarity), assuming constant Gamma distribution parameters with no covariates. Covariates are included in the models, in various configurations, following the schemes

Table 3
The results of MK test for the selected stations during 1980–2019 (alpha=5 %).

Station	Kendall's Tau	Var(S)	p-value (Two-tailed)	Sen's slope	Model interpretation
Pole-Baft	-0.317	11498930	< 0.00001	-0.01443	Reject H0
Meidan	-0.223	11498850	< 0.00001	-0.03289	Reject H0
Kenaroyeh	-0.184	11498940	< 0.00001	-0.09637	Reject H0

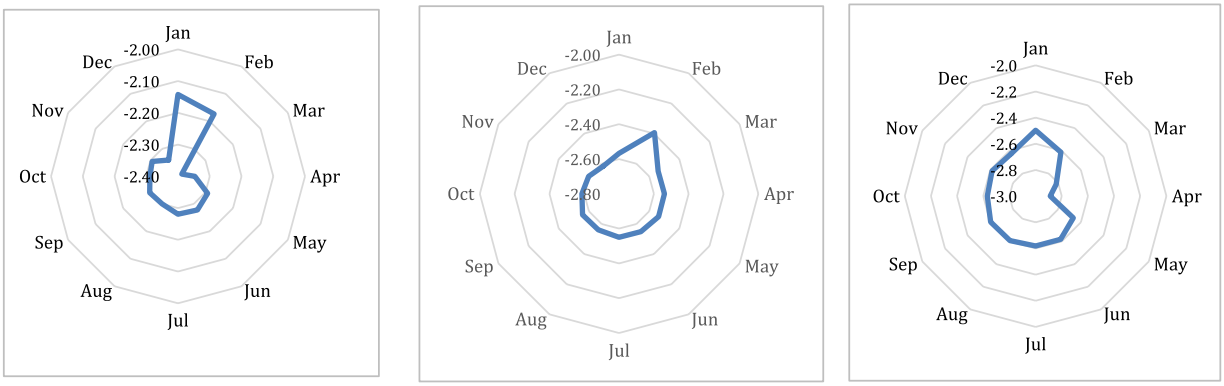

(a) Kenaroyeh (b) PoleBaft (c) Meidan

Fig. 4. Statistical results of the stationarity (ADF test) for cumulative runoff data in the study area, K= 12.

Table 4
Summary of AICs for stationary (M_0) and the NS Gamma models (M1, M2, M3) at PoleBaft station.

Model	Covariate	OCT	NOV	DEC	JAN	FEB	MAR	APR	MAY	JUN	JUL	AUG	SEP
M0	-	237	240	241	241	241	240	240	240	240	239	239	235
M11	P	226	227	237	239	239	225	220	219	218	222	225	225
M12	T	233	235	234	232	232	233	234	234	233	233	233	230
M13	PET	232	235	238	238	237	234	234	231	232	232	232	229
M14	R	207	200	201	195	196	202	206	185	184	187	192	205
M21	P-T	214	215	236	235	233	220	216	214	212	212	213	211
M22	P-PET	217	223	240	241	240	225	220	217	216	218	217	214
M23	P-R	209	203	204	198	197	202	192	187	188	191	195	207
M24	T-PET	233	235	238	236	236	235	235	231	230	232	234	229
M25	T-R	**201**	**188**	192	**181**	**190**	197	206	**179**	**177**	**179**	**184**	**194**
M26	PET R	205	198	199	189	195	194	200	183	185	187	190	199
M31	P- T- PET	217	219	239	238	236	223	220	217	215	216	216	213
M32	P-T-R	**201**	190	193	183	193	**175**	**183**	182	181	183	187	197
M33	T- PET-R	204	191	**190**	183	194	192	205	182	181	183	187	198
M34	P-PET-R	204	198	199	189	198	197	186	186	187	188	189	200

The smallest AIC value in each type of model is denoted in bold font.

presented in Tables 5–7 (one table for each of the three synoptic stations under study). In total, 15 model variants were tested to evaluate the influence of input factors on runoff dynamics. Models M11 through M14 correspond to NS frameworks incorporating a single covariate, whereas models M21 to M26 represent cases with two covariates. Additionally, models M31 to M34 denote NS models that include three covariates. The resulting AIC values corresponding to each fitted GAMLSS model for three hydrometric stations of PoleBaft, Meidan, and Kenaroyeh are presented in Tables 4, 5 and 6, respectively. The covariates considered in the model fits are different synoptic station data (T, P, PET, R). Lower AIC values indicate better model performance (i.e., a more parsimonious model that better fits the data without overfitting). Note, however, that slight differences in AIC (up to two units, according to rules of thumbs (Burnham and Anderson, 2004)) may not imply important differences in practice.

According to Table 4, the S model (M0) consistently exhibits higher AIC values compared to most NS models, suggesting relatively poor performance due to the lack of dynamic covariates. Among the evaluated NS models, Model M25, which incorporates T and R as covariates, demonstrates superior performance by yielding the lowest AIC values for nine months of the hydrological year—namely October, November, January, February, March, May, June, July, August and September. This pattern indicates that M25 is the most effective model for capturing hydrological drought dynamics under NS conditions at the Pol-Baft hydrometric station. Moreover, during the main drought season of the summer months (June, July, and August), Model M25 continues to demonstrate competitive performance, closely aligning with other high-performing models such as M32 and M33.

As shown in Table 5, Model M26, utilizing PET and R in its GAMLSS framework, consistently achieved the lowest AIC values for nine months (January-September). This indicates M26's capability of capturing NS hydrological drought at Meidan station. The strong performance of M26 suggests that the combined influence of PET and R effectively describes temporal variations in runoff distribution, yielding a more accurate and robust NS drought detection, superior to stationary (M0) and other NS models. Note, however, that AIC values are close to those of M25. Though, towards the end of the hydrological year, the differences in AIC are more pronounced.

Table 6 concerns Kenaroyeh, and like for previous site there is seasonal variability for the optimal NS model. Model M25 (T and R) was most frequently selected in the early/late hydrological year (October-January, April, September), which implies that T and R have critical influence. Conversely, Model M26 (PET and R) dominated summer (May-August). This intuitively reflects the influence of PET and R on runoff in warmer seasons. Note, again, that for some months the differences between NS models are slight. the findings of

Tables 4–6 demonstrate that the implementation of the GAMLSS framework at the three key hydrometric stations—PoleBaft, Meidan, and Kenaroyeh—revealed critical distinctions in runoff behavior under varying model specifications. The M0 yielded in all cases substantially higher AIC values, reflecting its limited capacity to accommodate underlying variability. In contrast, all NS models M1. – M3. which allow covariate-driven temporal shifts in the location and scale parameters of the Gamma distribution, achieved lower AICs, indicating improved goodness-of-fit. Among the tested configurations, the model incorporating non-stationarity in both location and scale parameters demonstrated superior performance. This underscores the methodological importance of simultaneously accounting for evolving central tendency and dispersion in streamflow behavior under NS climatic conditions.

Fig. 5 presents a comparative visualization of model performance between S and the best choices of the NS scenarios. The heat map displays ΔAIC values—computed as the difference in AIC scores between S and NS models—for the PoleBaft station, in conjunction with Baft, Jiroft, and Kahnooj covariates. Each cell represents the magnitude of ΔAIC for a specific month within the hydrological year (October–September), with warmer color intensities indicating stronger statistical preference for NS modeling configurations. These ΔAIC values function as diagnostic measures for evaluating model efficacy under time-varying covariate structures. Elevated values suggest that incorporating NS elements (in location, scale, or both) substantially improves runoff characterization, particularly in transitional periods such as late winter and early spring. This reinforces the rationale for adopting a flexible, climate-sensitive modeling framework in hydrological drought assessment.

As illustrated in Fig. 5, the Baft synoptic station consistently exhibited relatively higher values of ΔAIC for more than half of the hydrological year. In other words, the meteorological variables derived from the Baft station yielded superior model performance compared to those from the other synoptic stations. Therefore, Baft was selected as the representative station for further analysis and interpretation of the NS behavior of the SRI across the remaining hydrometric stations.

6.1. *A note on assessment of worm plots*

In this section, we discuss assessment of the fitted models, making use of so-called worm plots (Buuren and Fredriks, 2001). These could be seen as a detrended Q-Q plot of the residuals. The abscissa shows unit normal quantiles and the ordinate the difference between observed and expected quantiles (standardized residuals). As in conventional analysis of residuals, deviations should be minor and with no patterns. Using the implementation in R, 95 % confidence bands are displayed. We here present the scenarios for the three summer months July, August and September for each of the three hydrometric stations under study. In addition, we present the related AIC values.

In Fig. 6, top panel, we study PoleBaft. The fit is overall decent and satisfactorily. The worst case is the month of September, where a handful observations fall outside the confidence bands. This is not surprising when considering the AIC values – the AIC for September is considerably higher than for the other months, following the rules of thumbs for differences in AIC. Fig. 6, middle panel, displays the results for Meidan. Again, the fit is decent for July and August. In September, a wiggly S-curve pattern makes the fit less good. Finally, in Fig. 6 bottom panel, the worm plots for summer months at Kenaroyeh are displayed. The clouds of dots fall between the confidence bands for all months which is positive. The best fit is for July, while the other months show a tendency to wiggliness. AIC values support the interpretation, the lowest AIC (and hence best fit) being for July.

We conclude that interpretation of worm plots could have a degree of subjectiveness, but the conclusions are in line with corresponding AIC values. In some studies, e.g. Sun et al. (2020), worm plots are presented as a part of the model assessment. For our work, we draw from the cases presented above the conclusion that the AIC values serve as good indicators for the fit (as displayed in Tables 5–7).

6.2. *Estimation of the SSRI and the NSRI and drought characteristics*

Fig. 7 illustrates the 12-month SRI and NSRI time series spanning 1980–2019 across the three study stations, demonstrating a strong overall agreement in identifying major hydrological phases. Both indices—the SRI (black line) and NSRI (red line)—rise during periods of elevated runoff (wet conditions) and decline during runoff deficits (drought), confirming their mutual sensitivity to the underlying hydrological regime.

However, upon closer examination, notable discrepancies emerge, particularly under extreme events or sustained trends. These

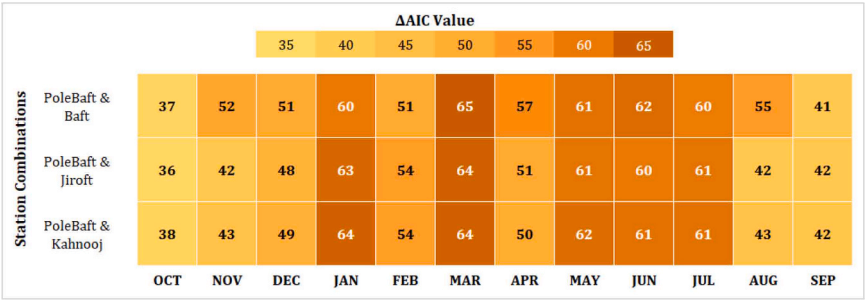

Fig. 5. ΔAIC Heatmap: Comparison of Stationary and Non-Stationary Model Performance Across Synoptic Station Combinations and Months.

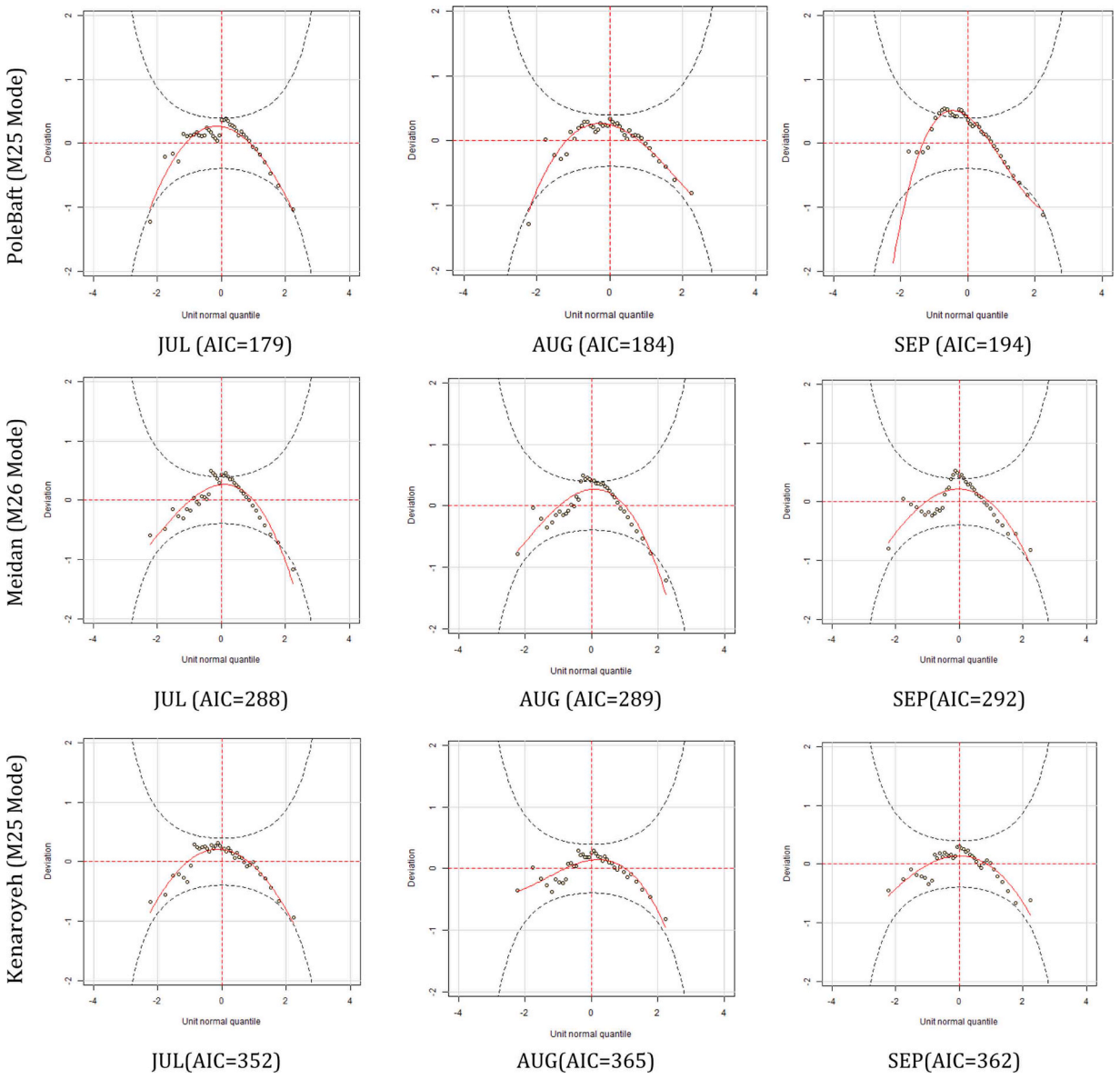

Fig. 6. Worm plots of summer months for the best scenario of each hydrometric station.

deviations underscore critical conceptual differences between the SRI and NSRI approaches to drought quantification. Although both indices encapsulate the same physical climate signals, their mathematical frameworks yield diverging assessments of drought severity and timing. These variations stem from the underlying assumptions: the SRI presumes temporal stability in hydrological processes, while the NSRI accounts for evolving climatic baselines—thereby offering a dynamic perspective on drought characterization under NS conditions.

At the Pole-Baft station, the time series in Fig. 7a illustrates notable periods of divergence between SRI and NSRI. For instance, during the severe drought period around 2008–2009, the SRI values plunge considerably lower, reaching below −3.0, indicating an exceptionally extreme drought event. In contrast, the NSRI values, while still negative, remain comparatively higher, suggesting a less severe drought when the evolving hydrological baseline is considered. Similar, albeit less pronounced, differences can be observed in the late 1990s, early 2000s, and again in 2017–2018. Conversely, during some wet periods, such as the early 1990s, the SRI peaks at slightly higher positive values than the NSRI.

The Meidan station, as depicted in Fig. 7b, exhibits overall patterns similar to Pole-Baft, yet with potentially different magnitudes of divergence between SRI and NSRI. For example, during the drought in the early 2000s and again around 2008–2009, the SRI consistently shows more pronounced negative values compared to the NSRI, indicating a perception of greater drought severity under stationary assumptions. Beyond magnitude, subtle shifts in the timing of peaks and troughs, or the rate of change, are discernible

Table 5
Summary of AICs for stationary (M_0) and the NS Gamma models (M1, M2, M3) at Meidan station.

Model	Covariate	OCT	NOV	DEC	JAN	FEB	MAR	APR	MAY	JUN	JUL	AUG	SEP
M0	-	352	352	352	352	352	351	352	352	352	352	352	352
M11	P	334	333	344	348	350	348	342	336	335	336	336	335
M12	T	345	345	344	345	344	344	342	342	343	343	343	344
M13	PET	342	342	344	347	348	346	343	340	341	341	341	342
M14	R	292	291	**286**	283	286	298	296	285	294	294	294	294
M21	P-T	337	337	345	347	345	347	341	337	337	338	338	337
M22	P-PET	337	337	346	350	349	350	344	338	338	338	338	337
M23	P-R	290	**288**	**286**	284	284	293	295	283	289	289	292	292
M24	T-PET	345	345	347	345	343	347	345	344	344	345	345	346
M25	T-R	**289**	291	288	278	282	288	295	282	292	294	294	294
M26	PET R	**289**	290	287	**277**	**278**	**288**	**293**	**277**	**285**	**288**	**289**	**292**
M31	P- T- PET	341	339	349	348	347	347	340	338	339	341	341	341
M32	P-T-R	**289**	289	289	281	283	292	297	283	289	291	293	293
M33	T- PET-R	292	293	291	280	282	288	295	280	289	292	293	295
M34	P-PET-R	292	291	290	280	282	291	296	281	289	291	293	294

The smallest AIC value in each type of model is denoted in bold font.

Table 6
Summary of AIC values for stationary (M_0) and the NS Gamma models (M1, M2, M3) at Kenaroyeh hydrometric station.

Model		OCT	NOV	DEC	JAN	FEB	MAR	APR	MAY	JUN	JUL	AUG	SEP
M0	**Covariate**	441	441	441	441	440	439	439	440	441	441	441	441
M11	-	423	422	428	434	438	432	425	424	424	424	423	423
M12	P	442	441	441	440	440	438	439	440	440	440	440	441
M13	T	437	438	441	440	440	437	436	433	433	434	434	434
M14	PET	365	359	363	367	399	392	388	368	363	361	370	366
M21	R	425	425	431	436	440	434	428	427	426	426	425	425
M22	P-T	424	424	431	435	441	435	428	425	423	423	423	423
M23	P-PET	365	**357**	**360**	363	**378**	386	388	366	362	359	368	365
M24	P-R	439	440	444	440	442	440	438	435	433	435	436	435
M25	T-PET	**360**	**357**	362	**360**	388	386	**386**	365	361	**356**	369	**362**
M26	T-R	365	359	362	362	389	389	**386**	**361**	**359**	**356**	**367**	365
M31	PET R	426	427	435	437	443	437	431	429	426	426	426	425
M32	P- T- PET	362	**357**	362	362	384	**381**	387	364	361	**356**	**367**	**362**
M33	P-T-R	363	361	365	363	390	388	388	362	362	359	371	365
M34	P-PET-R	367	360	363	365	390	384	390	364	363	360	368	367

The smallest AIC value in each type of model is denoted in bold font.

Table 7
Drought characteristics from the SSRI and the NSRI for three Hydrometric station in the study area.

	SSRI			
Station	**Number**	**Peak**	**Longest Duration (months)**	**Maximum severity**
PoleBaft	8	-3.77	96	-89.53
Meidan	10	-1.57	61	-26.61
Kenaroyeh	8	-1.86	100	-64.78
	NSRI			
Station	**Number**	**Peak**	**Longest Duration (months)**	**Maximum severity**
PoleBaft	9	-3.41	96	-87.64
Meidan	11	-2.04	61	-43.10
Kenaroyeh	9	-2.02	130	-101.13

between SRI and NSRI. One index might indicate a drought ending slightly earlier or later than the other, or a period of recovery commencing at a different point in time.

At the Kenaruyeh station, as shown in Fig. 7c, similar patterns of divergence between SRI and NSRI are observed, particularly during significant drought events like those around 2008–2009 and 2017–2018, where SRI consistently indicates more severe conditions than NSRI. While the general tendencies of divergence are consistent across all three stations, the degree and specific timing of these divergences appear to vary. For instance, the magnitude of the difference between SRI and NSRI during a particular drought event might be larger at one station than another, or the periods of most significant divergence might not perfectly align across all locations.

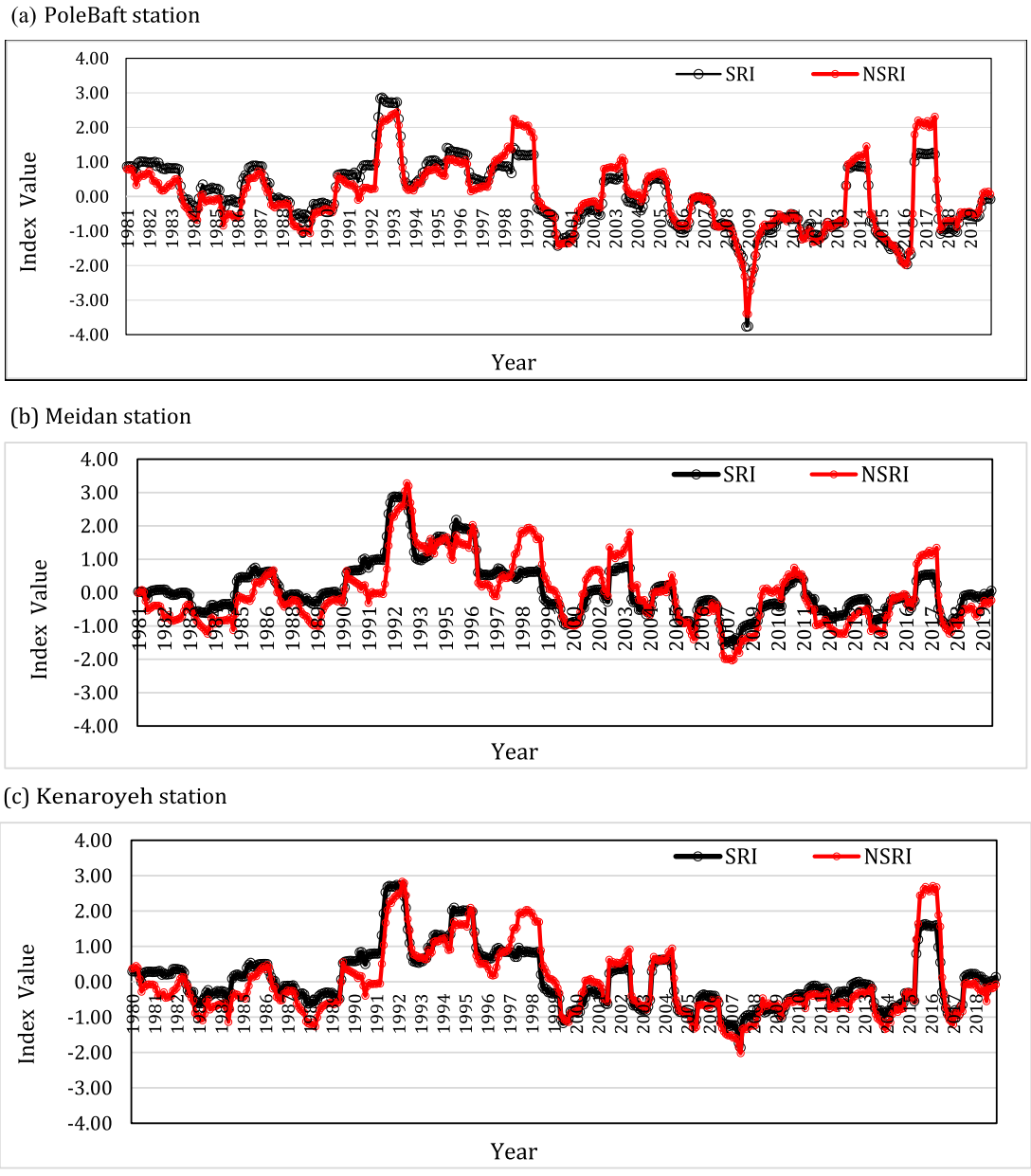

Fig. 7. 12-Month SSRI and NSRI series (1980–2019) at three locations (a) station PoleBaft (b) station Meidan (c) station Kenaroyeh.

6.3. Drought characteristics based on SSRI and NSRI

Table 7 presents key drought characteristics derived from the SSRI-12 and NSRI-12 time series at the Pole-Baft, Meidan, and Kenaroyeh stations. The analysis specifically examines three main attributes of drought events: peak intensity, duration, and severity. These characteristics were identified and extracted based on the run-length theory.

The drought peak is defined as the minimum value of the drought index within a given drought event, representing the event's maximum intensity. The duration refers to the time span from the onset to the end of the drought. Drought severity is quantified as the cumulative sum of the deviations of the drought index from a predefined threshold over the entire duration of the event (Yevjevich, 1967; Gu et al., 2019). In this study, a threshold of zero was adopted to delineate drought events.

As presented in Table 7, the analysis of the SRI time series at the Pole-Baft station over the 40-year study period reveals distinct patterns in hydrological drought behavior. Using run-length theory, eight drought events were identified, with the most intense event reaching a peak SRI value of –3.77, signifying an extreme hydrological deficit. The longest drought persisted for 96 months, while the highest severity recorded was –89.53. In comparison, the application of the NSRI, which accounts for NS situation in hydrological

processes, detected nine drought events. The most severe event under NSRI reached a peak value of –3.41, with a maximum drought severity of –87.64.

The Meidan station also identifies more drought events (11 events) based on the NSRI, while the drought peak (-2.04) and the maximum drought severity (-43.10) are higher than those from the SRI (-1.57 and −26.61). The longest drought durations are quite close from both the NSRI and the SRI for this station.

The Kenaroyeh station exhibited eight drought events under the SRI method, with the most extreme event recording a peak intensity of –1.86. The longest drought lasted 100 months, with a maximum severity of –64.78. Under the NSRI approach, the number of drought events increased to nine. Notably, the peak intensity became more severe at –2.02, and both the longest duration and maximum severity also increased significantly—reaching 130 months and –101.13, respectively.

A comparative analysis of drought characteristics at the Pole-Baft, Meidan, and Kenaroyeh stations reveals marked spatial variability and significant methodological divergence between the SRI and NSRI-12 approaches. At Pole-Baft, both indices consistently indicate prolonged and intense drought conditions, with a peak duration of 96 months and a marginal reduction in severity from –89.53 (SRI) to –87.64 (NSRI). In contrast, Meidan reflects milder droughts overall; however, the NSRI reveals heightened severity (–43.10 vs. –26.61) and intensity (–2.04 vs. –1.57), despite no change in maximum duration (61 months). The most pronounced shift occurs at Kenaroyeh, where NSRI captures an extension in drought duration from 100 to 130 months and a significant increase in severity from –64.78 to –101.13, underscoring the critical role of NS dynamics. Recall that Kenaroyeh is at the outlet of the basin, and in addition has the lowest elevation (1410 m) of the three stations.

6.4. Drought frequencies based on SSRI and NSRI

Fig. 8 illustrates drought occurrence frequencies (in %) for four drought categories—Mild, Moderate, Severe, and Extreme—based on both SRI and NSRI for three hydrometric stations: Pole-Baft, Meidan, and Kenaroyeh. This comparison reveals how the NS assumption affects drought characterization in different hydrological regimes.

According to Fig. 8, at the high-altitude Pole-Baft station (2270 m), the frequencies of drought categories derived from SRI and NSRI are closely aligned, with mild droughts dominating (∼40 %) and only marginal differences observed in moderate and severe drought categories. This suggests a relatively stationary hydrological regime with limited influence from evolving climate or anthropogenic factors. In contrast, the Meidan station (1915 m) shows a marked divergence between SRI and NSRI, with NSRI indicating a substantial increase in moderate (and to a lesser extent, severe) drought frequencies. This deviation implies the presence of NS likely driven by hydroclimatic variability or changing watershed conditions. The effect is even more pronounced at Kenaroyeh (1410 m), where NSRI reflects significantly higher frequencies of moderate and severe droughts compared to SRI. Given Kenaroyeh's downstream position and proximity to Jiroft Dam, these trends suggest the strong influence of human interventions such as dam regulation and agricultural water use.

7. Conclusions

Hydrological processes are increasingly influenced by climate variability and anthropogenic activities, challenging the reliability of traditional drought assessment methods. In the context of a non-stationary (NS) climate, it becomes essential to revisit and adapt drought indices, as key statistical properties such as mean and variability may no longer remain constant over time.

In this study, we introduced a Non-Stationary Standardized Runoff Index (NSRI) designed to more accurately capture hydrological drought dynamics in the Halil-Rud Basin, Iran. The NSRI is formulated using a NS Gamma distribution, where the location parameter is modeled as a function of time and hydro-climatic covariates. Model selection was conducted via forward selection within the Generalized Additive Models for Location, Scale, and Shape (GAMLSS) framework, offering a flexible and robust alternative to conventional statistical approaches such as the Mann-Kendall (MK) trend test.

Our findings highlight that the model incorporating nonstationarity in both the location and scale parameters consistently yielded superior performance, as determined by the Akaike Information Criterion (AIC). Although AIC values were often close among competing models, this dual-parameter approach provided a more nuanced understanding of drought variability. Worm plots were employed as diagnostic tools to evaluate model adequacy, particularly focusing on summer months when droughts tend to intensify. Among the three gauging stations analyzed, Pole-Baft, Meidan and Kenaroyeh, the poorest model fit was observed in September, suggesting greater model sensitivity during peak drought periods.

From a hydrological perspective, the NSRI results underscore spatial heterogeneity in drought conditions across the basin. At the upstream station (PolBaft), the limited influence of human activities was reflected in the NSRI outputs, whereas at the downstream station (Kenaroyeh), anthropogenic impacts—such as land use changes and water abstraction—were more pronounced. For instance, from Table 8, we find that SSRI identifies a total number of 26 droughts, while for NSRI the number is 29. The average peak for NSRI (-2,49) is higher compared to SSRI (-2.40). Considering the quantity of longest duration, only for the station of Kenaroyeh (at the outlet of the basin) a difference was found between the indices; the duration was 30 months longer with NSRI. Four our data, NSRI detected more draught episodes. These findings reinforce the importance of adopting non-stationary modeling approaches to account for evolving watershed conditions. Overall, the spatial pattern observed—from Pole-Baft to Kenaroyeh —indicates a gradient of increasing nonstationarity, emphasizing that traditional SSRI underrepresents drought severity and frequency in lower, more human-impacted regions. These findings highlight the importance of adopting nonstationary drought indices like NSRI for accurate drought risk assessment and informed water resources planning.

Our findings are relevant for the case study of Iran, but the framework offers a robust plan for policymakers to make use of NS

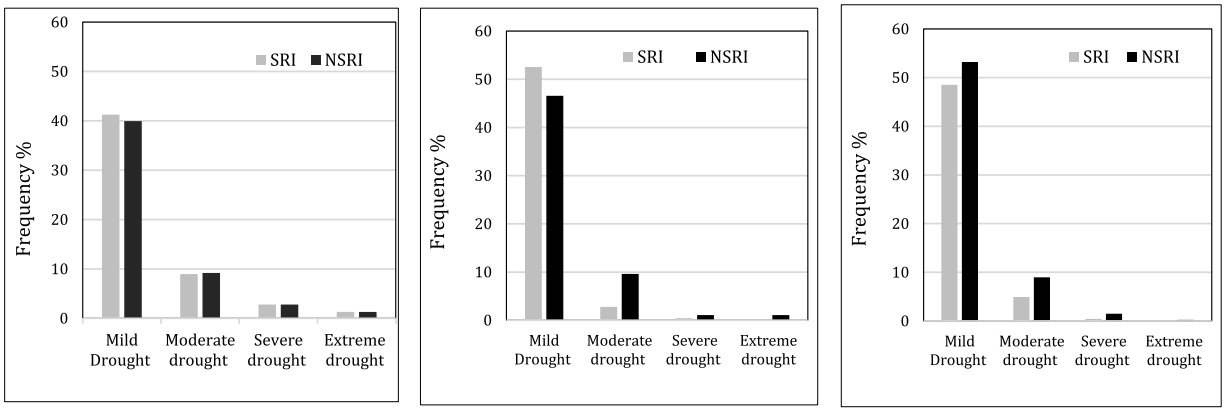

Fig. 8. Drought occurrence frequency based on SSRI and NSRI in the study area.

modeling into drought monitoring procedures. Hence, risk assessment and informing adaptive strategies for sustainable water resource management can be enhanced.

While both human activities and climate change influence the non-stationary behavior of droughts, the present study was limited by its reliance solely on hydroclimatic variables as covariates. Future research should incorporate large-scale climate drivers—such as the El Niño–Southern Oscillation (ENSO) and the North Atlantic Oscillation (NAO)—as well as indicators of human influence, including land-use change, to better quantify non-stationarity. Another promising direction involves exploring alternative two-parameter distributions beyond the conventional Gamma model originally proposed by Thom (1958). Particular attention could be given to distributions available within the GAMLSS framework, such as the lognormal distribution, which has been widely applied in drought studies and may yield complementary insights. Comparative evaluations of these models could improve understanding of performance and robustness across different settings. Finally, extending the analysis to additional case studies—such as coastal basins or regions characterized by contrasting climatic regimes—would further enhance the generalizability and applicability of the proposed methodology.

CRediT authorship contribution statement

Sedigheh Anvari: Writing – review & editing, Writing – original draft, Visualization, Validation, Supervision, Software, Resources, Project administration, Methodology, Formal analysis, Data curation, Conceptualization. **Ameneh Mianabadi:** Data curation. **Jesper Rydén:** Writing – review & editing, Writing – original draft, Supervision, Software, Methodology, Formal analysis, Conceptualization.

Funding

This research work was supported by the Graduate University of Advanced Technology (Institute of Science and High Technology and Environmental Science) (No. 1402/3641). The authors gratefully acknowledge this help.

Declaration of Competing Interest

The authors declare that they have no known competing financial interests or personal relationships that could have appeared to influence the work reported in this paper.

Acknowledgements

The authors gratefully acknowledge the support of the Graduate University of Advanced Technology, Institute of Science and High Technology and Environmental Science (Grant No. 1402/3641), which made this research possible.

Data Availability

Data will be made available on request.

References

Akaike, H., 1974. A new look at the statistical model identification. IEEE T Autom. Contr 19 (6), 716–723.

Anderson, M.C., Norman, J.M., Mecikalski, J.R., Otkin, J.A., Kustas, W.P., 2007. A climatological study of evapotranspiration and moisture stress across the continental United States based on thermal remote sensing: 1. Model formulation. J. Geophys. Res. Atmos. 112 (D10).

Anvari, S., Kim, J.H., Moghaddasi, M., 2019. The role of meteorological and hydrological uncertainties in the performance of optimal water allocation approaches. Irrig. Drain. 68 (2), 342–353.

Anvari, S., Moghaddasi, M., Bagheri, M.H., 2023. Drought mitigation through a hedging-based model of reservoir-farm systems considering climate and streamflow variations. Theor. Appl. Climatol. 152 (1), 723–737.

Anvari, S., Moghaddasi, M., 2024. Historical changes of extreme temperature in relation to soil moisture over different climatic zones of Iran. Stoch. Environ. Res. Risk Assess. 38 (1), 157–173. https://doi.org/10.1007/s00477-023-02558-2.

Anvari, S., Rydén, J., 2025. Estimation of return levels and associated uncertainties of extreme temperatures using a time-varying framework: a case study in Iran. Acta Geophys. https://doi.org/10.1007/s11600-025-01544-2.

Bazrafshan, J., 2017. Effect of air temperature on historical trend of long-term droughts in different climates of Iran. Water Resour. Manag. 31 (14), 4683–4698.

Bazrafshan, J., Cheraghalizadeh, M., Shahgholian, K., 2022. Development of a non-stationary standardized precipitation evapotranspiration index (NSPEI) for drought monitoring in a changing climate. Water Resour. Manag. 36 (10), 3523–3543.

Bazrafshan, J., Hejabi, S., 2018. A non-stationary reconnaissance drought index (NRDI) for drought monitoring in a changing climate. Water Resour. Manag. 32 (8), 2611–2624 (P).

Bonaccorso, B., Bordi, I., Cancelliere, A., Rossi, G., Sutera, A., 2003. Spatial variability of drought: an analysis of SPI in Sicily. Water Resour. Manag 17, 273–296.

Brown, J.F., Wardlow, B.D., Tadesse, T., Hayes, M.J., Reed, B.C., 2008. The Vegetation Drought Response Index (VegDRI): a new integrated approach for monitoring drought stress in vegetation. GISci. Remote Sens. 45 (1), 16–46.

Burnham, K.P., Anderson, D.R., 2004. Multimodel inference: understanding AIC and BIC in model selection. Sociol. Methods Res. 33 (2), 261–304.

Buuren, S.V., Fredriks, M., 2001. Worm plot: a simple diagnostic device for modelling growth reference curves. Stat. Med. 20, 1259–1277.

Dai, A., 2011. Characteristics and trends in various forms of the palmer drought severity index during 1900–2008. Clim. Dyn. 116 (D12).

Das, S., Das, J., Umamahesh, N.V., 2021. Nonstationary modeling of meteorological droughts: application to a region in India. J. Hydrol. Eng. 26 (2), 05020048.

Delavar, S., Anvari, S., Najafzadeh, M., Fathian, F., 2024. A review of stationary and non-stationary indices for drought monitoring in iran and other countries. Irrig. Water Eng. 14 (3), 175–193.

Dickey, D.A., Fuller, W.A., 1979. Distribution of the estimators for autoregressive time series with a unit root. J. Am. Stat. Assoc. 74 (366), 427–431.

Eslami, A., Anvari, S., Karimi, N., Mohamadi, S., 2022. Application of pixel-based and object-based approaches for LULC mapping in Jiroft region, SE Iran. ECOPERSIA 10 (1), 71–83.

Gan, T., et al. ,2023. [Title of Gan et al. paper]. Journal Name, Volume(Issue), pages. [Please insert full citation details.

Gu, J.S., Li, Q.F., Niu, M.Y., Chen, Q.H., He, P.F., Zhou, Z.M., Han, X.Y., 2019. An analysis of meteorological drought characteristics in the Upper Reaches of Huaihe River based on multidimensional copula function. China Rural Water Hydropower 61 (08), 83–87.

Guttman, N.B., 1998. Comparing the Palmer drought index and the standardized precipitation index. J. Am. Water Resour. Assoc. 34 (1), 113–121.

Guttman, N.B., 1999. Accepting the standardized precipitation index: a calculation algorithm 1. JAWRA J. Am. Water Resour. Assoc. 35 (2), 311–322.

Hao, Z., AghaKouchak, A., 2013. Multivariate standardized drought index: a parametric multi-index model. Adv. Water Resour. 57, 12–18.

Hastie, T., Tibshirani, R., 1987. Generalized additive models: some applications. J. Am. Stat. Assoc. 82 (398), 371–386.

Hayes, M.J., Svoboda, M.D., Wall, N., Widhalm, M., 2011. The Lincoln declaration on drought indices: universal meteorological drought index recommended. Bull. Am. Meteorol. Soc. 92, 485–488.

Heim Jr, R.R., 2002. A review of twentieth-century drought indices used in the United States. Bull. Am. Meteorol. Soc. 83 (8), 1149–1166 (P).

Huang, S., Huang, Q., Chang, J., Leng, G., 2016. Linkages between hydrological drought, climate indices and human activities: a case study in the Columbia River basin. Int. J. Climatol. 36 (1), 280–290.

Jiang, S., Wang, M., Ren, L., Xu, C.Y., Yuan, F., Liu, Y., Shen, H., 2019. A framework for quantifying the impacts of climate change and human activities on hydrological drought in a semiarid basin of Northern China. Hydrol. Process. 33 (7), 1075–1088.

Katz, R., 2010. Statistics of extremes in climate change. Clim. Change 100 (1), 71–76.

Li, L., Ngongondo, C.S., Xu, C.Y., Gong, L., 2013. Comparison of the global TRMM and WFD precipitation datasets in driving a large-scale hydrological model in southern Africa. Hydrol. Res. 44 (5), 770–788.

Li, J.Z., Wang, Y.X., Li, S.F., Hu, R., 2015. A nonstationary standardized precipitation index incorporating climate indices as covariates. J. Geophys. Res. Atmos. 120 (23), 12082–12095.

Liu, S., Huang, S., Xie, Y., Wang, H., Leng, G., Huang, Q., Wang, L., 2019. Identification of the non-stationarity of floods: changing patterns, causes, and implications. Water Resour. Manag. Int. J. Publ. Eur. Water Resour. Assoc. (EWRA) 33 (3), 939–953.

Mahmodzadeh, E., Anvari, S., 2021. Verification of estimated evapotranspiration by surface energy balance algorithm for land and the information of OLI and TIRS sensors. Watershed Eng. Manag. 13 (1), 150–159 (in Persian).

Mann, H.B., 1945. Nonparametric tests against trend. Econometrica 13, 245–259. https://doi.org/10.2307/1907187.

McKee, T.B., Doesken, N.J., Kleist, J., 1993. The relationship of drought frequency and duration to time scales. Proc. 8th Conf. Appl. Climatol. 17 (22), 179–183.

Mishra, A.K., Singh, V.P., 2009. Analysis of drought severity-area-frequency curves using a general circulation model and scenario uncertainty. J. Geophys. Res.: Atmos. 114 (D6).

Mishra, A.K., Singh, V.P., 2010. A review of drought concepts. J. Hydrol. 391 (1-2), 202–216.

Mitchell, T.D., Jones, P.D., 2005. An improved method of constructing a database of monthly climate observations and associated high-resolution grids. Int. J. Climatol. A J. R. Meteorol. Soc. 25 (6), 693–712.

Moghaddasi, M., Anvari, S., Akhondi, N., 2022. A trade-off analysis of adaptive and non-adaptive future optimized rule curves based on simulation algorithm and hedging rules. Theor. Appl. Climatol. 148 (1), 65–78. https://doi.org/10.1007/s00704-022-03930-y.

Mohammadi, T., Moghaddasi, M., Anvari, S., Aziz, R., 2024. Estimation of non-stationary return levels of extreme temperature by CMIP6 models. Water Pract. Technol. 19 (2), 594–610.

Morid, S., Smakhtin, V., Moghaddasi, M., 2006. Comparison of seven meteorological indices for drought monitoring in Iran. Int. J. Climatol. 26 (7), 971–985.

Naderi, K., Moghaddasi, M., Shokri, A., 2022. Drought occurrence probability analysis using multivariate standardized drought index and copula function under climate change. Water Resour. Manag. 36 (8), 2865–2888.

New, M., Hulme, M., Jones, P., 1999. Representing twentieth-century space–time climate variability. Part I: development of a 1961–90 mean monthly terrestrial climatology. J. Clim. 12 (3), 829–856.

Palmer, D.S., 1965. Sequencing jobs through a multi-stage process in the minimum total time—a quick method of obtaining a near optimum. J. Oper. Res. Soc. 16 (1), 101–107.

Pasho, E., Camarero, J.J., de Luis, M., Vicente-Serrano, S.M., 2011. "Impacts of drought at different time scales on forest growth across a wide climatic gradient in north-eastern Spain. Agric. For. Meteorol. 151 (12), 1800–1811.

Rashid, M.M., Beecham, S., 2019. Characterization of meteorological droughts across South Australia. Meteorol. Appl. 26 (4), 556–568.

Raziei, T., Bordi, I., Pereira, L.S., 2008. A precipitation-based regionalization for Western Iran and regional drought variability. Hydrol. Earth Syst. Sci. 12 (6), 1309–1321.

Rigby, R.A. & Stasinopoulos, D.M. ,2001. The GAMLSS project: a flexible approach to statistical modelling. In: New Trends in Statistical Modelling: Proceedings of the 16th International Workshop on Statistical Modelling (B. Klein & L. Korsholm, eds). Odense, pp. 249–256.

Rigby, R.A., Stasinopoulos, D.M., 2005. Generalized additive models for location, scale and shape. J. R. Stat. Soc. Ser. C. (Appl. Stat.) 54 (3), 507–554.

Russo, S., Dosio, A., Sterl, A., Barbosa, P., Vogt, J., 2013. Projection of occurrence of extreme dry-wet years and seasons in Europe with stationary and nonstationary Standardized Precipitation Indices. J. Geophys. Res. Atmos. 118 (14), 7628–7639.
Rydén, J., 2019. A note on analysis of extreme minimum temperatures with the GAMLSS framework. Acta Geophys. 67, 1599–1604.
Sarhadi, A., Burn, D.H., Concepcion Ausin, M., Wiper, M.P., 2016. Time-varying nonstationary multivariate risk analysis using a dynamic Bayesian copula. Water Resour. Res. 52 (3), 2327–2349 (P).
Shukla, S., Wood, A.W., 2008. Use of a standardized runoff index for characterizing hydrologic drought. Geophys. Res. Lett. 35 (2). L02405.
Stasinopoulos, D.M., Rigby, R.A., 2007. Generalized additive models for location scale and shape (Gamlss) in R. J. Stat. Softw. 23 (1), 1–46.
Sun, X., Li, Z., Tian, Q., 2020. Assessment of hydrological drought based on nonstationary runoff data. Hydrol. Res. 51 (5), 894–910.
Thom, H.C., 1958. A note on the gamma distribution. Mon. Weather Rev. 86, 117–122.
Tsakiris, G., Vangelis, H.J.E.W., 2005. Establishing a drought index incorporating evapotranspiration. Eur. Water 9 (10), 3–11.
Vicente-Serrano, S.M., Beguería, S., López-Moreno, J.I., 2010. A multisca lar drought index sensitive to global warming: the standardized precipitation evapotranspiration index. J. Clim. 23 (7), 1696–1718.
Villarini, G., Serinaldi, F., Smith, J.A., Krajewski, W.F., 2009. On the stationarity of annual flood peaks in the continental United States during the 20th century. Water Resour. Res. 45 (8).
Wang, Y., Li, J., Feng, P., Hu, R., 2015. A time-dependent drought index for non-stationary precipitation series. Water Resour. Manag 29, 5631–5647.
Wilhite, D.A., 2000. Drought preparedness and response in the context of Sub-Saharan Africa. J. Contingencies Crisis Manag. 8 (2), 81–92 (P).
Xiong, L., Guo, S., 2004. Trend test and change-point detection for the annual discharge series of the Yangtze River at the Yichang hydrological station/Test de tendance et détection de rupture appliqués aux séries de débit annuel du fleuve Yangtze à la station hydrologique de Yichang. Hydrol. Sci. J. 49 (1), 99–112.
Yevjevich, V.M., 1967. An objective approach to definitions and investigations of continental hydrologic droughts, 23. Colorado State University, Fort Collins, CO, USA, p. 25.